AIP | Applied Physics Letters

On the mechanism of recombination at oxide precipitates in silicon

J. D. Murphy, K. Bothe, V. V. Voronkov, and R. J. Falster

Citation: Appl. Phys. Lett. **102**, 042105 (2013); doi: 10.1063/1.4789858
View online: http://dx.doi.org/10.1063/1.4789858
View Table of Contents: http://apl.aip.org/resource/1/APPLAB/v102/i4
Published by the American Institute of Physics.

On the mechanism of recombination at oxide precipitates in silicon

J. D. Murphy,[1,a)] K. Bothe,[2,b)] V. V. Voronkov,[3,c)] and R. J. Falster[1,3,d)]
[1]*Department of Materials, University of Oxford, Parks Road, Oxford OX1 3PH, United Kingdom*
[2]*Institut für Solarenergieforschung Hameln/Emmerthal, Am Ohrberg 1, 31860 Emmerthal, Germany*
[3]*MEMC Electronic Materials, viale Gherzi 31, 28100 Novara, Italy*

(Received 15 November 2012; accepted 15 January 2013; published online 30 January 2013)

Oxide precipitates are well known to degrade minority carrier lifetime in silicon, but the mechanism by which they act as recombination centres is not fully understood. We report minority carrier lifetime measurements on oxide precipitate-containing silicon which has been intentionally contaminated with iron. Analysis of the injection-dependence of lifetime demonstrates the same recombination centres exist in iron-contaminated and not intentionally contaminated samples, with the state density scaling with iron loss from the bulk. This shows that recombination activity arises from impurity atoms segregated to oxide precipitates and/or surrounding crystallographic defects. © *2013 American Institute of Physics*. [http://dx.doi.org/10.1063/1.4789858]

Recombination of electrons and holes at defects limits the efficiency of photovoltaics, the vast majority of which are made from single-crystal Czochralski silicon (Cz-Si) or multicrystalline silicon (mc-Si). Both materials typically contain 10^{17} to $10^{18}\,\mathrm{cm}^{-3}$ of oxygen which can precipitate during crystal growth and processing.[1–6] Oxide precipitates typically form unintentionally in vacancy-rich regions in rapidly pulled Cz-Si[5] and at crystallographic defects in mc-Si.[2,3] Precipitation of oxygen is generally undesirable for photovoltaics as it increases recombination,[7–20] but it is often desirable in silicon for microelectronics as precipitates and surrounding defects (dislocations and stacking faults) can confine device-ruining metallic contaminants away from active regions in internal gettering processes.[21,22]

Although it has long been known that the precipitation of oxygen introduces recombination centres,[7–20] after at least 35 years of research, the physical origin of these centres is not fully understood. Oxygen precipitation creates so-called P_b dangling bonds.[16,18] These defects can act as recombination centres,[18] but as they are readily passivated by hydrogen[23,24] they may not give rise to a substantial reduction in the minority carrier lifetime of a processed silicon solar cell. It is well established that very low concentrations of transition metal impurities strongly increase the recombination activity of dislocations in silicon.[25,26] It has also been observed that electron beam induced contrast in the vicinity of oxide precipitates dramatically increases when they are decorated by iron.[13,14] In this letter, we aim to understand and quantify the effect of iron contamination on recombination at oxide precipitates and associated defects. This is important both for understanding the fundamental physics of the recombination mechanism and for parameterising carrier lifetime in photovoltaics made from low cost silicon feedstocks in which oxide precipitates will be decorated.

Our methodology is to use injection-dependent lifetime spectroscopy[27] to study recombination in oxide precipitate-containing silicon which has been intentionally post-contaminated with iron. Our previous study in material which had not been intentionally contaminated (referred to henceforth as "uncontaminated" samples) revealed an approximately linear relationship between overall recombination rate and precipitate *density*, i.e., recombination is essentially independent of precipitate size.[17] A more detailed analysis of the injection-dependence of the minority carrier lifetime shows the recombination can be parameterised in terms of two independent Shockley-Read-Hall (SRH) centres.[19] We use a linear formulation of SRH statistics in which the electron lifetime due to a defect in a p-type semiconductor varies with $X = n/p$ (where n and p are the total electron and hole concentrations, respectively) according to[19,28]

$$\tau_n = \frac{1}{\alpha_n N}\left[1 + \frac{Qn_1}{p_0} + \frac{p_1}{p_0} + X\left(Q - \frac{Qn_1}{p_0} - \frac{p_1}{p_0}\right)\right], \quad (1)$$

where α_n is the capture coefficient (the product of thermal velocity and capture cross-section) for electrons, $Q = \alpha_n/\alpha_p$, where α_p is the capture coefficient for holes, and p_0 is the equilibrium hole concentration. The SRH densities are given by $n_1 = N_C \exp\left(-\frac{E_C - E_T}{kT}\right)$ and $p_1 = N_V \exp\left(-\frac{E_T - E_V}{kT}\right)$, where N_C and N_V are the density of states in the conduction band and valence band, respectively, and E_T is the energy level of the defect. As their precise physical origin is not yet understood, the two states found in oxide precipitate-containing silicon are referred to simply as "Defect 1" and "Defect 2." Defect 1 has $Q_1 = 157$ at room temperature and is at $E_V + 0.22\,\mathrm{eV}$. Defect 2 has $1/Q_2 = 1200$ at room temperature and is at $E_C - 0.08\,\mathrm{eV}$.[19] In this present letter, we use the formulation of SRH statistics given by Eq. (1) to extract values of $\alpha_n N$ for states present in iron-contaminated specimens.

Samples were prepared from 150 mm diameter high-purity p-type Cz-Si wafers with a boron concentration of $1.3 \pm 0.2 \times 10^{15}\,\mathrm{cm}^{-3}$ and an initial oxygen concentration (DIN50438/I) of $7.7 \pm 0.2 \times 10^{17}\,\mathrm{cm}^{-3}$ (low) or $9.1 \times 10^{17}\,\mathrm{cm}^{-3}$ (high). Wafers were subjected to a four stage-thermal treatment described in Ref. 17. Different concentrations of strained oxide precipitates ($N_{strained}$) were created by varying nucleation and growth times. Concentrations were

a)john.murphy@materials.ox.ac.uk.
b)bothe@isfh.de.
c)vvoronkov@memc.it.
d)rfalster@memc.it.

determined by chemical etching and ranged from 1.5×10^6 to $4.5 \times 10^{10}\,\mathrm{cm}^{-3}$. A TEM investigation revealed samples in which dislocations, and in some cases stacking faults, surrounded some of the oxide precipitates.[29] Transition metal contamination was achieved by rubbing the back-sides of 5 cm by 5 cm samples with iron pieces (99.95% purity from Testbourne Limited, UK). Samples were then annealed in air in a pre-heated furnace at temperatures from 690 to 775 °C for times chosen to ensure complete iron diffusion through the sample. Although our intention was to contaminate samples only with iron, the possibility that other transition metal impurities have entered the samples cannot be completely ruled out. Unless otherwise stated, cooling was rapid, with the samples removed from the furnace at temperature and placed on a heat sink. It is estimated that rapidly cooled samples were cooled to below ~100 °C in <10 s. Contaminated samples were subjected to an HF dip, an RCA clean, and silicon nitride surface passivation using remote plasma enhanced chemical vapour deposition. The passivation scheme used involved the samples being at 400 °C for ~10 min and has previously been shown to give a surface recombination velocity below 10 cm/s.[30] It is likely that the silicon nitride growth process introduces bulk hydrogen,[31] which may passivate P_b dangling bond centres.[23,24]

Minority carrier lifetime was measured by quasi-steady-state photoconductance[32] using a Sinton WCT-120 lifetime tester. Prior to testing, samples were subjected to a 200 °C anneal for >10 min to dissociate boron-oxygen defects.[33] Samples were then subjected to >50 pulses of light with a ~10 μs decay constant from a Quantum Qpaq-X flash lamp placed very close to the sample to dissociate iron-boron pairs[34] and an initial lifetime measurement was made with the iron in the interstitial state. A final lifetime measurement was then made >24 h later, by which time the FeB pairs had re-formed. The bulk iron concentration was determined from the characteristic lifetime change,[34–36] using methods detailed in Refs. 17 and 37. The minority carrier lifetime measured with the iron in the interstitial state was corrected for band-to-band, Coloumb-enhanced Auger, and recombination at interstitial iron using corrections detailed in Ref. 17. The resulting residual lifetime, τ_{residual}, therefore represents the best estimate we are able to obtain for the lifetime due to impurity-decorated oxide precipitates and associated defects.

Figure 1 shows residual minority carrier lifetime plotted against $X = n/p$ for an uncontaminated sample, and also samples with a range of precipitate densities which have been post-contaminated with iron. Remarkably, in all cases, the injection-dependence agrees with a linear superposition of the reciprocal lifetimes for Defect 1 and Defect 2 using the SRH parameters given earlier. For different precipitate densities and contamination conditions, the fits differ only because the product of the capture coefficient for electrons and the state density ($\alpha_n N$) is chosen to fit the experimental data. Figure 2 shows data for samples from the same wafer (hence similar precipitate densities and sizes) which were subjected to iron contamination anneals at different temperatures. Again the same two sets of defect parameters can be used to fit the data in all cases, with the $\alpha_n N$ values in some way dependent on the iron contamination temperature. For all oxide precipitate-containing samples studied (with and

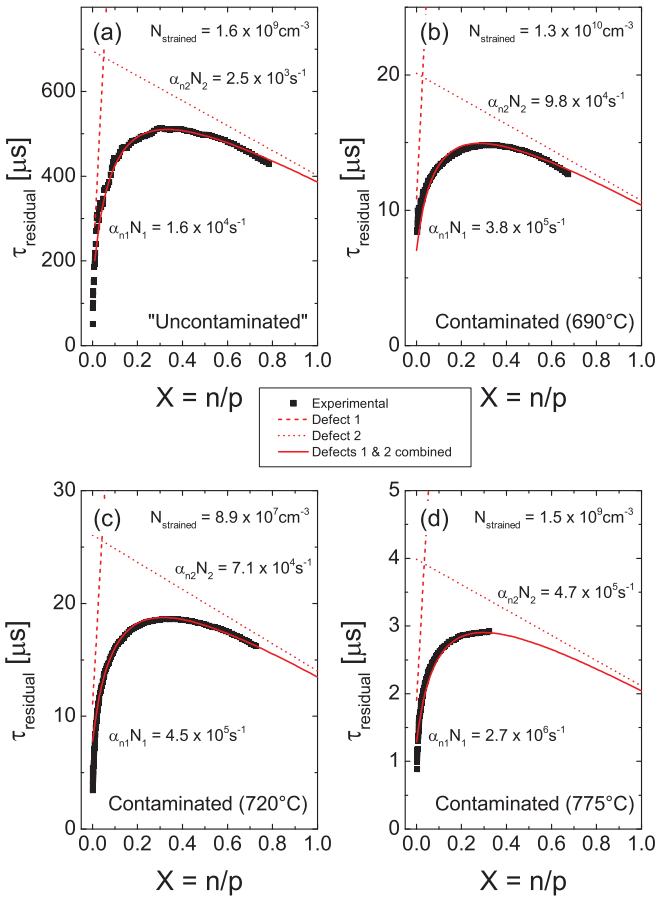

FIG. 1. Injection-dependent lifetime measurements in low oxygen oxide precipitate-containing samples which have (a) not been intentionally contaminated; and (b) to (d) been contaminated with iron at the temperature shown followed by a rapid cool. Dislocations and stacking faults were found to surround the precipitates in sample (b), but not the other samples. All the experimental data can be fitted using the same two defects, with the $\alpha_n N$ parameters stated.

without intentional iron contamination), the ratio of $\alpha_{n1}N_1$ to $\alpha_{n2}N_2$ is approximately constant at between ~3 and ~8.

Figure 3 shows the bulk iron concentrations measured in a range of iron-contaminated samples. In precipitate-free material, our contamination procedure gives the iron solubility as $[Fe_{solubility}] = 1.3 \times 10^{21} \exp\left(-\frac{1.8\,\mathrm{eV}}{kT}\right) \mathrm{cm}^{-3}$, where T is

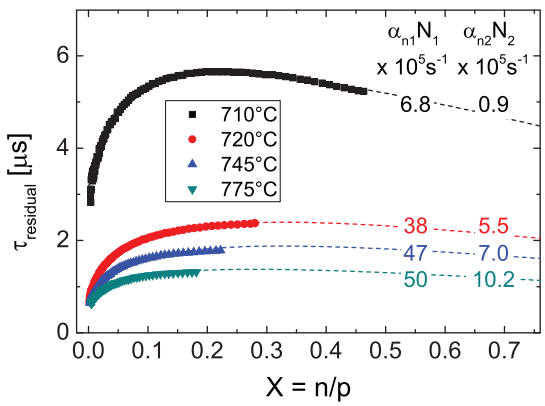

FIG. 2. Residual minority carrier lifetime versus $X = \frac{n}{p}$ for low oxygen samples containing oxide precipitates rubbed with iron and heated to different temperatures followed by a rapid cool. The concentration of strained precipitates is $1.2 \times 10^9\,\mathrm{cm}^{-3}$ in all cases.

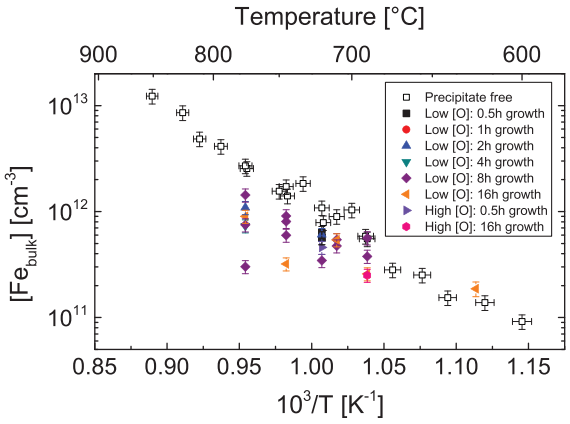

FIG. 3. Bulk iron concentrations measured in specimens with and without pre-existing oxide precipitates contaminated with iron followed by a rapid cool. Within experimental error, the bulk iron concentration is the same, or lower, in specimens containing oxide precipitates.

the contamination temperature.[37,38] The bulk iron concentration in precipitate-containing samples is usually substantially lower (and never significantly higher) than in precipitate-free specimens, as iron segregates to the precipitates and surrounding defects. There appears to be no clear relationship between the final bulk iron concentrations and the precipitate growth time (which determines the precipitate size). There is however a clear relationship between the iron segregated to the precipitates and the recombination rate determined from the injection-dependent lifetime measurements. The number of iron atoms at the precipitates, ΔFe, is assumed to be given by the difference between the solubility and the measured iron remaining in the bulk, $[Fe_{bulk}]$, i.e.,

$$\Delta Fe = [Fe_{solubility}] - [Fe_{bulk}]. \quad (2)$$

Figure 4 shows the relationship between the $\alpha_n N$ parameter per strained precipitate and ΔFe per strained precipitate for samples in which dislocations, and in some cases, stacking faults were found to surround the precipitates. This relationship is linear for Defect 1 and Defect 2. We therefore conclude that the number of segregated iron atoms determines the recombination activity of the strained oxide precipitates and surrounding defects.

The solubility of iron in silicon is dependent on temperature,[37,38] so the total concentration of iron in a given sample is dependent upon the contamination temperature. However, interstitial iron is highly mobile at the contamination temperatures used,[39] and, even for the rapid cooling conditions used, significant iron transport occurs during cooling. Figure 5 shows lifetime data for two samples from the same oxide precipitate-containing wafer contaminated at the same temperature (745 °C), but cooled at different rates. The slower cooling rate was still sufficiently rapid to avoid significant iron diffusion to the iron silicide phase present at the surface and the re-establishment of equilibrium.[38] As before, the established parameters for Defect 1 and Defect 2 provide excellent fits to the lifetime data. The $\alpha_n N$ parameters are larger in the case of the slow cooled specimen, which is because more iron has decorated the precipitates upon cooling than in the rapidly cooled specimen. Small random differences in cooling rate for the rapidly cooled specimens

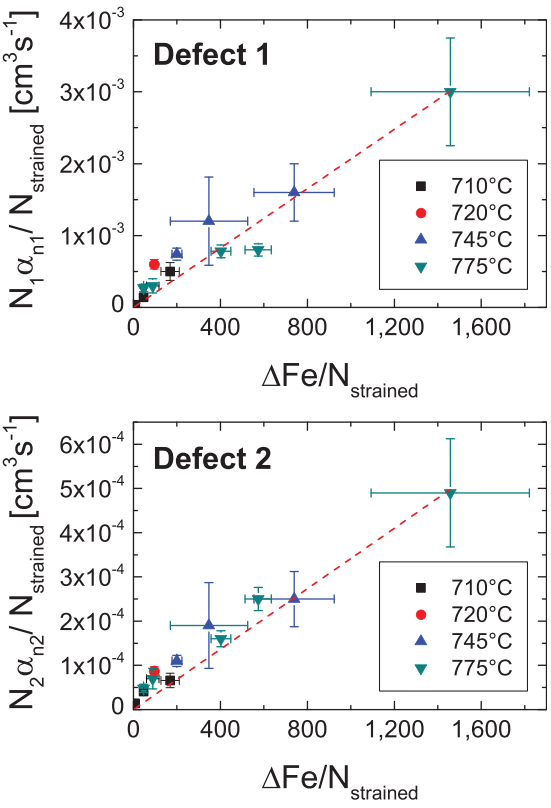

FIG. 4. The SRH parameter $\alpha_n N$ per strained precipitate for both defects plotted against the iron lost from the bulk given by Eq. (2) per precipitate. The data shown are for low oxygen specimens in which dislocations, and in some cases, stacking faults surround the precipitates.

may have therefore resulted in differences in the decoration level of oxide precipitates and associated defects, but this is accounted for by correlating the iron lost from the bulk with the recombination activity (Figure 4).

The recombination activity of iron-decorated oxide precipitates can be parameterised in terms of the same two recombination centres which have previously been associated with "uncontaminated" precipitates.[19] The (additional) iron decorating the precipitates increases the $\alpha_n N$ parameter for each defect in a way which correlates approximately

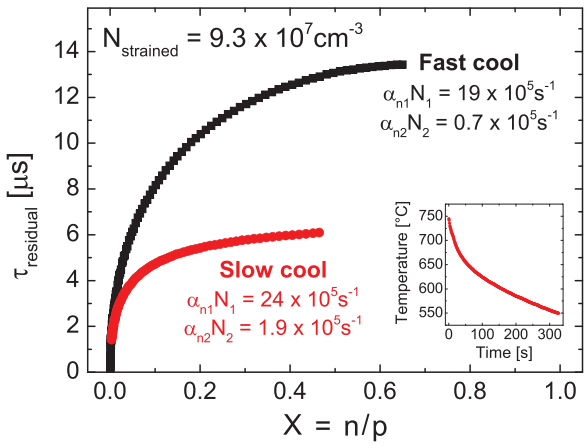

FIG. 5. Injection-dependent lifetime measurements in low oxygen oxide precipitate-containing samples contaminated with iron at 745 °C. The higher lifetime sample was subjected to the usual rapid cool. The lower lifetime sample experienced the temperature profile shown in the inset, followed by a rapid cool from 550 °C to room temperature.

linearly with bulk iron lost to the precipitates. The capture coefficient for electrons and state density are inherently coupled. The strong correlation between iron loss from the bulk and the $\alpha_n N$ parameters (Figure 4) can be explained by variation of the density of recombination centres. Thus, both Defect 1 and Defect 2 appear to be associated with iron segregated to oxide precipitates and surrounding defects, and the measured $\alpha_n N$ parameter is proportional to the concentration of iron segregated to the precipitates. Linear correlation between ΔFe per precipitate and $\alpha_n N$ per precipitate suggests that atomic decoration of iron (rather than precipitation) is responsible for the recombination activity in these samples.

For specimens which were not intentionally contaminated, the recombination rate via both independent defects varies approximately linearly with precipitate density, with $N_1\alpha_{n1}/N_{strained} = 2.9 \times 10^{-5}\,cm^3\,s^{-1}$ and $N_2\alpha_{n2}/N_{strained} = 5.1 \times 10^{-6}\,cm^3\,s^{-1}$.[19] The linear relationship in Figure 4 suggests the recombination activity of the "uncontaminated" specimens is consistent with each strained precipitate being decorated with just 10 to 20 atoms of iron. This implies the absolute capture coefficients for electrons at the two defects are $\alpha_{n1} = 2 \pm 1 \times 10^{-6}\,cm^3\,s^{-1}$ and $\alpha_{n2} = 4 \pm 2 \times 10^{-7} cm^3\,s^{-1}$. These values are substantially larger than bulk interstitial iron for which $\alpha_n = 7.2 \times 10^{-8}\,cm^3\,s^{-1}$.[36] This highlights the importance of avoiding oxygen precipitation (and subsequent contamination) in silicon materials for photovoltaics. In both "uncontaminated" and contaminated samples, the recombination rate is approximately dependent upon precipitate density (not size). An explanation for this is that iron segregates to regions of the precipitates whose number is invariant with size, such as in the vicinity of precipitate corners.

Even under the most carefully controlled modern conditions, it is not surprising that oxide precipitates are decorated by low levels of metal impurities. The iron concentration at the precipitates required for the electrical activity seen in "uncontaminated" samples is much less than the solubility at temperatures at which oxide precipitates are typically nucleated and grown[37,39] and at which solar cells are processed. The detection limit for iron contamination of silicon surfaces is $\sim 1 \times 10^9\,cm^{-2}$, and such contamination levels would be sufficient to decorate oxide precipitates in Cz-Si to the required level (especially given the multiple thermal cycles used for the precipitation treatment). After a 10 s thermal treatment at 800 °C, Haunschild *et al.* found a strong enhancement of the recombination activity of concentric rings formed of oxide precipitates in Cz-Si for photovoltaics.[4] Their thermal process would have been sufficient to redistribute low concentrations of bulk iron in the material, resulting in increased iron decoration of the precipitates. The proposed impurity-mediated recombination mechanism can explain why solar cells made from single-crystal silicon containing oxide precipitates can result in an efficiency reduction of 4% (absolute).[4] In mc-Si, transition metal contamination from the crucible and lining materials[40] mean that oxide precipitates are likely to be decorated.

In summary, this letter shows that iron atoms segregated to oxide precipitates and surrounding defects give rise to recombination. The states introduced have the same SRH parameters as previously assigned to "uncontaminated" precipitates,[19] which suggest the electrical activity of these is also impurity-related. This is similar in part to recombination at dislocations.[25,26] There is an important difference, however, insofar as dangling bonds have also been associated with oxide precipitates,[16,18] but not generally with dislocations.[41,42] Thus, it appears that iron decoration of oxide precipitates and associated defects introduces new recombination centres, in addition to those associated with dangling bonds.

The authors thank D. Gambaro, M. Cornara, and M. Olmo (MEMC Electronic Materials) for performing precipitation treatments and characterization, and P. R. Wilshaw (University of Oxford) for helpful discussions. J.D.M. is the recipient of a Royal Academy of Engineering/EPSRC Research Fellowship and an EPSRC First Grant (EP/J01768X/1).

[1]W. Bergholz, M. J. Binns, G. R. Booker, J. C. Hutchison, S. H. Kinder, S. Messoloras, R. C. Newman, R. J. Stewart, and J. G. Wilkes, Philos. Mag. B **59**, 499 (1989).
[2]H. J. Möller, C. Funke, A. Lawerenz, S. Riedel, and M. Werner, Sol. Energy Mater. Sol. Cells **72**, 403 (2002).
[3]K. Bothe, K. Ramspeck, D. Hinken, C. Schinke, J. Schmidt, S. Herlufsen, R. Brendel, J. Bauer, J.-M. Wagner, N. Zakharov, and O. Breitenstein, J. Appl. Phys. **106**, 104510 (2009).
[4]J. Haunschild, I. E. Reis, J. Geilker, and S. Rein, Phys. Status Solidi (RRL) **5**, 199 (2011).
[5]P. K. Kulshreshtha, Y. Yoon, K. M. Youssef, E. A. Good, and G. Rozgonyi, J. Electrochem. Soc. **159**, H125 (2012).
[6]M. Tajima, Y. Iwata, F. Okayama, H. Toyota, H. Onodera, and T. Sekiguchi, J. Appl. Phys. **111**, 113523 (2012).
[7]L. C. Kimerling, H. J. Leamy, and J. R. Patel, Appl. Phys. Lett. **30**, 217 (1977).
[8]K. H. Yang, H. F. Kappert, and G. H. Schwuttke, Phys. Status Solidi A **50**, 221 (1978).
[9]M. Miyagi, K. Wada, J. Osaka, and N. Inoue, Appl. Phys. Lett. **40**, 719 (1982).
[10]S. S. Chan, C. J. Varker, J. D. Whitfield, and R. W. Carpenter, Mater. Res. Soc. Symp. Proc. **46**, 281 (1985).
[11]J. M. Hwang and D. K. Schroder, J. Appl. Phys. **59**, 2476 (1986).
[12]J. Vanhellemont, E. Simoen, A. Kaniava, M. Libezny, and C. Claeys, J. Appl. Phys. **77**, 5669 (1995).
[13]W. Seifert, M. Kittler, M. Seibt, and A. Buczkowski, Solid State Phenom. **47–48**, 365 (1996).
[14]F. G. Kirscht, Y. Furukawa, W. Seifert, K. Schmalz, A. Buczkowski, S. B. Kim, H. Abe, H. Koya, and J. Bailey, Mater. Sci. Eng., B **36**, 230 (1996).
[15]T. Mchedlidze, K. Matsumoto, and E. Asano, Jpn. J. Appl. Phys. **38**, 3426 (1999).
[16]M. Koizuka and H. Yamada-Kaneta, J. Appl. Phys. **88**, 1784 (2000).
[17]J. D. Murphy, K. Bothe, M. Olmo, V. V. Voronkov, and R. J. Falster, J. Appl. Phys. **110**, 053713 (2011).
[18]V. Lang, J. D. Murphy, R. J. Falster, and J. J. L. Morton, J. Appl. Phys. **111**, 013710 (2012).
[19]J. D. Murphy, K. Bothe, R. Krain, V. V. Voronkov, and R. J. Falster, J. Appl. Phys. **111**, 113709 (2012).
[20]K. Bothe, R. J. Falster, and J. D. Murphy, Appl. Phys. Lett. **101**, 032107 (2012).
[21]R. J. Falster and W. Bergholz, J. Electrochem. Soc. **137**, 1548 (1990).
[22]D. Gilles, E. R. Weber, and S. Hahn, Phys. Rev. Lett. **64**, 196 (1990).
[23]M. Koizuka and H. Yamada-Kaneta, J. Appl. Phys. **84**, 4255 (1998).
[24]E. Cartier, J. H. Stathis, and D. A. Buchanan, Appl. Phys. Lett. **63**, 1510 (1993).
[25]T. S. Fell, P. R. Wilshaw, and M. D. de Coteau, Phys. Status Solidi A **138**, 695 (1993).
[26]V. Kveder, M. Kittler, and W. Schröter, Phys. Rev. B **63**, 115208 (2001).
[27]S. Rein, *Lifetime Spectroscopy: A Method of Defect Characterization in Silicon for Photovoltaic Applications* (Springer, Berlin, 2005).
[28]V. V. Voronkov, R. Falster, J. Schmidt, K. Bothe, and A. V. Batunina, ECS Trans. **33**(11), 103 (2010).

[29]R. Falster, V. V. Voronkov, V. Y. Resnik, and M. G. Milvidskii, in *High Purity Silicon VIII: Proceedings of the Electrochemical Society* (2004), Vol. 200405, p. 188.
[30]T. Lauinger, J. Moschner, A. G. Aberle, and R. Hezel, J. Vac. Sci. Technol. A **16**, 530 (1998).
[31]A. G. Aberle, Sol. Energy Mater. Sol. Cells **65**, 239 (2001).
[32]R. A. Sinton and A. Cuevas, Appl. Phys. Lett. **69**, 2510 (1996).
[33]K. Bothe and J. Schmidt, J. Appl. Phys. **99**, 013701 (2006).
[34]G. Zoth and W. Bergholz, J. Appl. Phys. **67**, 6764 (1990).
[35]D. H. Macdonald, L. J. Geerligs, and A. Azzizi, J. Appl. Phys. **95**, 1021 (2004).
[36]S. Rein and S. W. Glunz, J. Appl. Phys. **98**, 113711 (2005).
[37]J. D. Murphy and R. J. Falster, Phys. Status Solidi (RRL) **5**, 370 (2011).
[38]J. D. Murphy and R. J. Falster, J. Appl. Phys. **112**, 113506 (2012).
[39]A. A. Istratov, H. Hieslmair, and E. R. Weber, Appl. Phys. A **69**, 13 (1999).
[40]T. Buonassisi, A. A. Istratov, M. D. Pickett, J. P. Rakotoniaina, O. Breitenstein, M. A. Marcus, S. M. Heald, and E. R. Weber, J. Cryst. Growth **287**, 402 (2006).
[41]J. R. K. Bigger, D. A. McInnes, A. P. Sutton, M. C. Payne, I. Stich, R. D. King-Smith, D. M. Bird, and L. J. Clarke, Phys. Rev. Lett. **69**, 2224 (1992).
[42]R. Jones, Mater. Sci. Eng., B **71**, 24 (2000).